JACS
JOURNAL OF THE AMERICAN CHEMICAL SOCIETY
Communication
pubs.acs.org/JACS

# Completely Miscible Polyethylene Nanocomposites

Matthias Bieligmeyer,[†] Sara Mehdizadeh Taheri,[†] Ian German,[‡] Christophe Boisson,[‡] Christian Probst,[⊥] Wolfgang Milius,[∥] Volker Altstädt,[§] Josef Breu,[∥] Hans-Werner Schmidt,[⊥] Franck D'Agosto,[‡] and Stephan Förster*,[†]

[†]Physikalische Chemie I, [§]Polymer Engineering, [∥]Anorganische Chemie I, and [⊥]Makromolekulare Chemie I, Universität Bayreuth, Universitätsstrasse 30, 95440 Bayreuth, Germany

[‡]Université de Lyon, Univ. Lyon 1, CPE Lyon, CNRS UMR 5265 Laboratoire de Chimie, Catalyse, Polymères et Procédés (C2P2), Equipe LCPP, Bat 308F, 43 Bd du 11 novembre 1918, F-69616 Villeurbanne, France

Supporting Information

**ABSTRACT:** A route to fully miscible polyethylene (PE) nanocomposites has been established based on polymer-brush-coated nanoparticles. These nanoparticles can be mixed with PE at any ratio, with homogeneous dispersion, and without aggregation. This allowed a first systematic study of the thermomechanical properties of PE nanocomposites without interference from aggregation effects. We observe that the storage modulus in the semicrystalline state and the softening temperature increase significantly with increasing nanoparticle content, whereas the melt viscosity is unaltered by the presence of nanoparticles. We show that the complete miscibility with the semicrystalline polymer matrix and the improvement of thermomechanical properties in the solid state is caused by the PE-coated nanoparticles being nucleating agents for the crystallization of PE. This provides a general route to fully miscibility nanocomposites with semicrystalline polymers.

Polymer nanocomposites have gathered substantial academic and industrial interest since the first reports in the early 1990s.[1−3] Observations of large property changes at very low-volume fractions of added nanoparticles and the possibility to incorporate nanoparticles with specific properties providing new functionality have motivated an increasing number of investigations. Further progress in the area of nanocomposites has been limited by the strong tendency of nanoparticles to aggregate in polymeric matrices.[4] To achieve highly dispersed states in nanocomposites, *in situ* polymerization[5] and kinetic entrapment[6] techniques have been exploited. However, only a full thermodynamic compatibilization of the nanoparticles to provide miscibility with the polymer matrix makes the production of nanocomposites independent of the preparation procedure and provides long-term thermodynamic stability.

In order to prepare nanoparticles that are miscible with the polymer matrix, the nanoparticle surface has to be covered with a layer of a matrix-miscible polymer. Generally, this is still insufficient to provide complete miscibility, due to the loss of conformational entropy of the matrix polymers close to the nanoparticle surface.[7] Due to the large specific surface area of nanoparticles, this purely entropic effect alone already leads to immiscibility and aggregation. We have recently discovered that coating of nanoparticles with a spherical polymer brush layer provides miscibility, because the low polymer segment density at the periphery of the brush layer allows for sufficient conformational freedom for the matrix polymer chains.[8]

Complete miscibility has until now been demonstrated only for polystyrene nanocomposites. Polystyrene is a convenient noncrystalline amorphous polymer that commonly serves as a first model system. A much greater challenge for nanoparticle/polymer miscibility is the preparation of polyolefin nanocomposites. Most polyolefins are semicrystalline and are phase separated into crystalline and amorphous domains which likely promotes inhomogeneous nanoparticle distribution and aggregation. In addition the attachment of a spherical polymer brush layer requires well-defined end-functionlized polyolefins, which have until recently not been readily accessible.

Methods for the preparation of nanocomposites with polyethylene (PE), a ubiquitous commodity polymer, have previously been investigated. Besides melt-blending, the immobilization of Ziegler−Natta-type catalysts on nanoparticle surfaces[9−11] and *in situ* nanoparticle synthesis[12] has been reported. Both methods have their limitations with respect to achievable maximum volume fractions without aggregation, the homogeneity of the nanoparticle distribution in the polymer matrix, and the variability in nanoparticle type and quality, which is mostly limited to silica nanoparticles.

For the present study we focused on PE iron oxide nanoparticle nanocomposites, as iron oxide nanoparticles: (1) represent an important class of nanoparticles, (2) provide additional functionality, i.e., magnetic properties, and (3) represent a synthetic challenge, as a stable attachment to polyolefins has not yet been demonstrated. For the attachment we chose a ligand exchange procedure, which had been used for the attachment of polystyrenes to a variety of chemically different nanoparticles.[8] As an appropriate coordinatively binding polymer chain-end we selected primary amino groups.

Narrowly disperse PEs with primary amino end groups were until recently difficult to prepare via conventional PE synthesis routes. A solution to this issue of low molecular weight PE was developed via catalyzed chain growth (CCG) polymerization of ethylene in toluene at 80 °C using a neodymocene precatalyst $[Cp^*_2NdCl_2Li(OEt_2)_2]$ ($Cp^* = C_5Me_5$) and butyloctylmagnesium as an activator/chain-transfer agent (CTA).[13,14] The living

**Received:** July 31, 2012
**Published:** October 19, 2012



dx.doi.org/10.1021/ja307297c | J. Am. Chem. Soc. 2012, 134, 18157−18160

characteristics of the polymer chain growth allow accurate control over molecular weight by variation of CTA loading and ethylene consumption. Magnesium-bound PE with $M_n$ = 1400 Da was prepared by this route and quenched with iodine to give PE-I with 95% of polymer chains iodo-end-capped as determined by $^1$H NMR spectroscopy. The end-group was modified according to an established procedure[15,16] by nucleophilic substitution with sodium azide and the resultant PE-$N_3$ reduced with lithium aluminum hydride to produce PE-$NH_2$ with 95% of chains amino-terminated.

The amino-functionalized PE chains were attached to the maghemite nanoparticles via a ligand exchange process. In this process oleic acid, which is the stabilizing layer on the surface of the nanoparticles during and after their synthesis, is replaced by amino end-functionalized PE. Oleic acid-stabilized nanoparticles and an excess of $\alpha$-amino PE were dissolved in 1,2,4-trichlorobenzene at 130 °C, then left to cool to room temperature to precipitate the nanoparticle/PE nanocomposite and separate it from free oleic acid by centrifugation. Subsequent dissolution in 1,2,4-trichlorobenzene at 130 °C followed by slow cooling allows a size-selective sequential precipitation to separate the PE-coated nanoparticles (they phase-separate first) from the free PE chains. The nanoparticle weight fractions of samples of the PE-coated nanoparticles were determined by thermogravimetric analysis (TGA) and were found to be in the range of 30−40%. More detailed TGA results can be found in the Supporting Information (SI).

As a matrix polymer for the nanocomposites, we chose a commercial low-density polyethylene (LDPE) LUPOLEN to demonstrate the relevance of the PE brush layer nanocomposites to possible applications. To prepare the LDPE nanocomposites, the PE-coated nanoparticles and the LDPE matrix polymer were dissolved in a 1,2,4-trichlorobenzene at 130 °C. The solution was cooled, inducing the precipitation of nanoparticles and PE to form the nanocomposite. By variation of the nanoparticle/free polymer ratio, nanocomposites with different weight fractions of nanoparticles were prepared.

The distribution of nanoparticles within the nanocomposites was characterized by transmission electron microscopy (TEM). Nanocomposite samples were prepared for analysis by drop-casting of dilute, hot solutions onto a TEM grid. We first examined the pure PE-coated nanoparticles, as they can be considered the PE nanocomposites with the highest weight fraction of nanoparticles. As shown in Figure 1a, we observe a rhombic crystal morphology typical for PE crystals. Within the crystal, nanoparticles are homogeneously distributed, with no aggregation (Figure 1b).

PE nanocomposites with lower nanoparticle concentrations, between 1 and 7.4 wt %, were investigated in more detail. We observe that upon cooling and precipitation from hot 1,2,4-trichlorobenzene solutions, the nanocomposites form stable, submicrometer-size, spherical colloidal particles as shown in Figure 1c. The particle sizes were measured by dynamic light scattering (detailed results in SI) and were found to decrease with increasing nanoparticle loading. Homogeneous distribution of nanoparticles within each particle was apparent from TEM images (Figure 1d), demonstrating the miscibility of the PE-coated nanoparticles with the PE matrix.

The unprecedented preparation of fully miscible PE nanocomposites enabled the investigation of changes in polymer thermomechanical properties upon addition of nanoparticles without interference from the effects of nanoparticle aggregation. Dynamic mechanical analysis of the

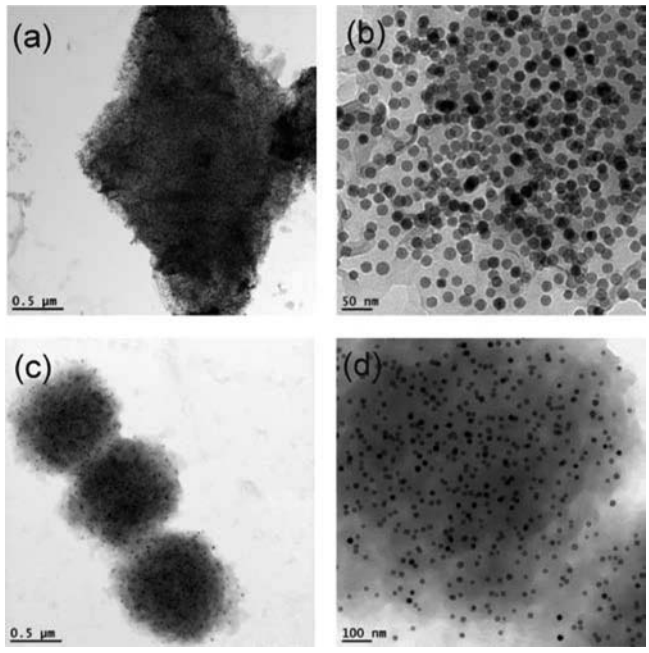


**Figure 1.** Electron micrographs of a highly filled rhombic PE nanocomposite crystal (54 wt % nanoparticles) (a) with homogeneous distribution of nanoparticles (b) and of spherical nanocomposite particles for a nanoparticle loading of 7.4 wt % at low (c) and high (d) magnification.

nanocomposites was carried out in the temperature range of 80−140 °C, which encompasses PE softening and melting transition.

Figure 2 shows the storage and loss moduli, $G'$ and $G''$, at a frequency of 1 Hz over a temperature range of 80−140 °C. At

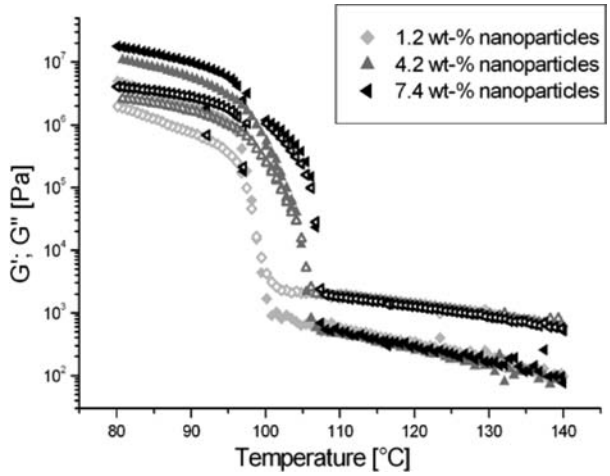


**Figure 2.** Storage ($G'$, solid symbols) and loss ($G''$, hollow symbols) moduli of LDPE nanocomposites as a function of temperature for different loading fractions of nanoparticles. Oscillation frequency was $\omega$ = 1 rad/s.

temperatures of up to 95 °C the nanocomposites are in the solid state, where $G' \gg G''$. Substantial increases in nanocomposite storage modulus ($G'$) from that of unmodified LDPE are observed with increasing nanoparticle loading, up to a factor of 10 for the nanocomposite with 7.4 wt % nanoparticles. Similarly, a significant influence of nanoparticle incorporation on the softening temperature was evident. From


dx.doi.org/10.1021/ja307297c | J. Am. Chem. Soc. 2012, 134, 18157−18160

pure PE, with a softening temperature of 98 °C, increasing nanoparticle loading leads to a systematic increase of the softening temperature, up to 108 °C for the 7.4 wt % nanocomposite.

At temperatures >110 °C we observe the melt-phase behavior, where $G'' \gg G'$. Surprisingly, the rheological properties of the molten nanocomposites were found to be independent of nanoparticle presence or weight fraction. This is in contrast to previous reports of increases in $G'$ and $G''$ by a factor of 2 observed upon nanoparticle loading.[17,18] To determine the effect of the frequency chosen for the measurements in Figure 2, we measured $G'$ and $G''$ at a temperature of 120 °C over the complete frequency range of 0.1−100 rad/s (see SI). No effect of nanoparticle presence on the rheological properties of molten PE was observed at any oscillation frequency.

Our experiments demonstrate that nanoparticles coated with a PE brush layer are fully miscible with a semicrystalline PE matrix. The nanoparticles are homogeneously distributed throughout the polymer matrix, even at the highest nanoparticle weight fractions and after extended thermal treatment in the melt (Figure S7), with no indication of a preferential location in either crystalline or amorphous regions. This had not been expected, similarly as the changes in the thermomechanical properties with significant increases in storage modulus and softening temperature in the solid state but no effect on the melt viscosity.

To obtain further insight, we performed DSC experiments for nanocomposites with increasing nanoparticle loading. As shown in Figure 3, the pure LDPE matrix has a melting

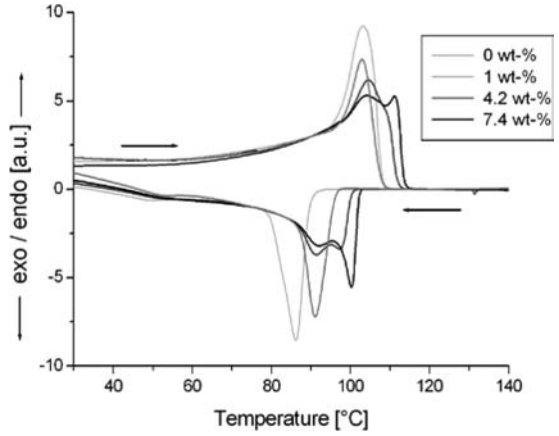


**Figure 3.** DSC heating and cooling curves (second heating/first cooling cycles) for neat PE (0%) and nanocomposites with increasing nanoparticle loading (1, 4.2, 7.4 wt %).

temperature of 103 °C. Upon addition of 4.2 wt % of nanoparticles, a noticeable fraction of the nanocomposites melts at higher temperatures, up to 110 °C. A further increase of the nanoparticle content leads to the appearance of a clearly observable second melting peak at a higher temperatures (111 °C for the highest loading ratio of 7.4 wt %), whose relative peak area increases with increasing nanoparticle content. The DSC heating curves thus parallel the findings in the dynamic mechanical experiments where the softening temperature was similarly increased.

The cooling curves in Figure 3 show that pure LDPE has a crystallization temperature of 86 °C. For the 1 wt % (0.2 vol %) nanocomposite, the crystallization temperature is shifted to 91°, whereas the melting temperature is unaffected. This is a characteristic feature of nucleation. For 4.7 wt % nanoparticle content the crystallization peak splits into two peaks with a crystallization temperature of 91 °C for the lower temperature and 100 °C higher temperature. Further increasing the nanoparticle content increases the relative peak area of the high-temperature peak, which also narrows.

The DSC measurements indicate that low-volume fraction PE-coated nanoparticles act as nucleating agents for PE. At higher volume fractions they induce the formation of a higher melting crystalline PE phase. Their ability to form PE crystals has already been described in relation to Figure 1a,b. It well explains their homogeneous distribution in the semicrystalline PE matrix as observed in Figure 1c,d. The changes in crystallinity cause the observed strong increase of the storage modulus in the solid state and the increase in the melting temperature as shown in Figure 2. It also explains the absence of any rheological effects in the melt state, as at low-volume fraction of nanoparticles they have negligible effect on the flow behavior of the highly viscous LDPE melt. We note that a 7.4 wt % fraction of $Fe_2O_3$ nanoparticles corresponds to only 1.4 vol %, which is quite small.

As seen by the XRD patterns in Figure 4, the crystal structure of the LDPE matrix is not affected by the presence of the

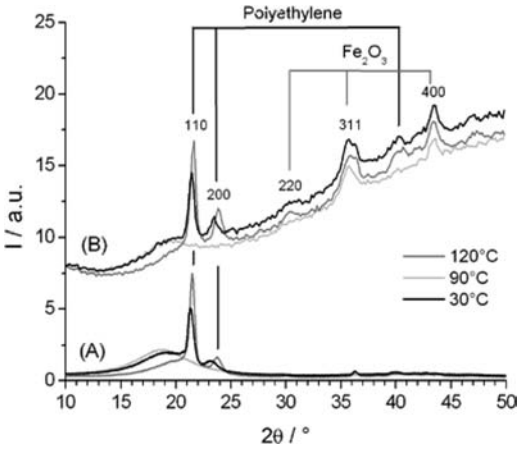


**Figure 4.** XRD pattern measured for the neat LDPE (A) and the 7.4 wt % nanocomposite (B) at different temperatures in the solid state (30°, 90 °C) and in the molten state (120 °C). Indexed are the reflections of PE and $\gamma$-$Fe_2O_3$.

nanoparticles. The PE in the neat LDPE and in the nanocomposite shows the same diffraction patterns in the solid state (30° and 90 °C) and the same amorphous halo in the melt state (120 °C). The nanocomposite shows additional reflections due to the presence of the nanoparticles, which are indexed for $\gamma$-$Fe_2O_3$ in Figure 4.

In summary we demonstrate the complete miscibility and stable homogeneous dispersion of PE brush layer-coated nanoparticles within a PE matrix. This enabled the preparation of highly and homogeneously filled PE nanocomposites with variable nanoparticle loadings. The addition of nanoparticles leads to a large increase of the storage modulus and the softening temperature of the solid polymer but does not alter the melt-phase rheological properties of the PE, which is highly desirable for applications and processing. We find that the homogeneous distribution in the semicrystalline polymer matrix and the improved thermomechanical properties in the


dx.doi.org/10.1021/ja307297c | J. Am. Chem. Soc. 2012, 134, 18157−18160

solid state is due to PE-coated nanoparticles being a nucleation agent for PE, as deduced from the DSC experiments. We thus show for the first time that polymer brush-layer coatings provide a versatile route to an efficient and homogeneous dispersion of any kind of nanoparticles in semicrystalline polymers.

## ■ ASSOCIATED CONTENT

### Supporting Information

Detailed descriptions of materials and methods used. This material is available free of charge via the Internet at http://pubs.acs.org.

## ■ AUTHOR INFORMATION

### Corresponding Author

stephan.foerster@uni-bayreuth.de

### Notes

The authors declare no competing financial interest.

## ■ ACKNOWLEDGMENTS

The help of Denise Barelmann-Kahlbohm and Sascha Ehlert with preparing the microtomed sections and TEM micrographs is greatly appreciated. We also wish to thank the Basell Polyolefine GmbH for the free supply of PE.

M.B. likes to thank the Elite Network of Bavaria for the support of his studies. I.G. thanks the University Claude Bernard Lyon 1 and S.F. the SFB 840 for financial support.

## ■ REFERENCES

(1) Usuki, A.; Kojima, Y.; Kawasumi, M.; Okada, A.; Fukushima, Y.; Karauchi, T.; Kamigaito, O. *J. Mater. Res.* **1993**, *8*, 1179.
(2) Vaia, R. A.; Ishii, H.; Giannelis, R. A. *Chem. Mater.* **1993**, *5*, 1649.
(3) Lan, T. P.; Pinnavaia, T. J. *Chem. Mater.* **1994**, *6*, 2216.
(4) Vaia, R. A.; Wagner, H. D. *Mater. Today* **2004**, *7*, 32.
(5) Lu, Y.; Yang, A.; Sellinger, A.; Lu, M.; Huang, J.; Fan, H.; Haddad, R.; Lopez, G.; Burns, A. R.; Sasaki, D. Y.; Shelnutt, J.; Brinker, J. *Nature* **2001**, *410*, 913.
(6) Liff, S. M.; Kumar, N.; McKinley, G. H. *Nat. Mater.* **2007**, *6*, 65.
(7) de Gennes, P. G. *Scaling Concepts in Polymer Physics*; Cornell University Press: Ithaca, New York, 1979.
(8) Fischer, S.; Salcher, A.; Kornowski, A.; Weller, H.; Forster, S. *Angew. Chem., Int. Ed. Engl.* **2011**, *50*, 7811−7814.
(9) McNally, T.; Pötschke, P.; Halley, P.; Murphy, M.; Martin, D.; Bell, S. E. J.; Brennan, G. P.; Bein, D.; Lemoine, P.; Quinn, J. P. *Polymer* **2005**, *46*, 8222−8232.
(10) Wang, T.-L.; Ou, C.-C.; Yang, C.-H. *J. Appl. Polym. Sci.* **2008**, *109*, 3421−3430.
(11) Monteil, V.; Stumbaum, J.; Thomann, R.; Mecking, S. *Macromolecules* **2006**, *39*, 2056.
(12) Zhu, J.; Wei, S.; Li, Y.; Sun, L.; Haldolaarachchige, N.; Young, D. P.; Southworth, C.; Khasanov, A.; Luo, Z.; Guo, Z. *Macromolecules* **2011**, *44*, 4382−4391.
(13) Pelletier, J. F.; Mortreux, A.; Olonde, X.; Bujadoux, K. *Angew. Chem., Int. Ed.* **1996**, *35*, 1854.
(14) Mazzolini, J.; Espinosa, E.; D'Agosto, F.; Boisson, C. *Polymer Chemistry* **2010**, *1*, 793.
(15) Briquel, R.; Mazzolini, J.; Le Bris, T.; Boyron, O.; Boisson, F.; Delolme, F.; D'Agosto, F.; Boisson, C.; Spitz, R. *Angew. Chem., Int. Ed.* **2008**, *47*, 9311.
(16) Damiron, D.; Mazzolini, J.; Cousin, F.; Boisson, C.; D'Agosto, F.; Drockenmuller, E. *Polym. Chem* **2012**, *3*, 1838.
(17) Guo, N.; DiBenedetto, S. A.; Kwon, D.-K.; Wang, L.; Russell, M. T.; Lanagan, M. T.; Facchetti, A.; Marks, T. J. *J. Am. Chem. Soc.* **2007**, *129*, 766−767.
(18) Qin, Y.; Wang, N.; Zhou, Y.; Huang, Y.; Niu, H.; Dong, J. Y. *Macromol. Rapid Commun.* **2011**, *32*, 1052−1059.